A robust SARS-CoV-2 replication model in primary human epithelial cells at the air liquid interface to assess antiviral agents

Thuc Nguyen Dan Do[1], Arnab K. Chatterjee[2], Philippe A. Gallay[3], Michael D. Bobardt[3], Laura Vangeel[1], Steven De Jonghe[1], Johan Neyts[1], Dirk Jochmans[1]

[1] KU Leuven - Department of Microbiology, Immunology and Transplantation, Rega Institute, Laboratory of Virology and Chemotherapy, Leuven, Belgium.

[2] CALIBR - Department of Medicinal Chemistry, the Scripps Research Institute, La Jolla, CA, USA.

[3] CALIBR - Department of Immunology and Microbial Science, the Scripps Research Institute, La Jolla, CA, USA.

Email: johan.neyts@kuleuven.be and dirk.jochmans@kuleuven.be

ABSTRACT

There are, besides Remdesivir (RDV), no approved antivirals for the treatment and/or prophylaxis of SARS-CoV-2 infections. To aid in the search for antivirals against this virus, we explored the use of human tracheal airway epithelial cells (HAEC) and human small airway epithelial cells (HsAEC) grown at the air/liquid interface (ALI) and infected at the apical side with either one of two different SARS-CoV-2 isolates. The virus was shown to replicate to high titers for extended periods of time (at least 8 days) and, in particular an isolate with the D614G in the spike (S) protein did so more efficiently at 35°C than at 37°C. The effect of a selected panel of reference drugs that were added to the culture medium at the basolateral side of the system was explored. GS-441524 (the parent nucleoside of Remdesivir), EIDD-1931 (the active metabolite of Molnupiravir) and IFN (β1 and λ1) all resulted in a dose-dependent inhibition of viral RNA and infectious virus titers at the apical side. However, AT-511 (a guanosine nucleotide previously reported to inhibit SARS-CoV-2) failed to inhibit viral replication. Together, these results provide a reference for further studies aimed at selecting SARS-CoV-2 inhibitors for further preclinical and clinical development.

KEY WORDS

SARS-CoV-2, antivirals, primary human airway epithelial cells, HAEC, GS-441524, EIDD-1931, AT-511, IFN

INTRODUCTION

Besides Remdesivir (RDV), there are no approved antivirals for the treatment and/or prophylaxis of SARS-CoV-2 infections, although the clinical benefit of RDV is still a matter of debate[1]. Major efforts are ongoing to develop novel antiviral drugs. To aid in their development physiological relevant models are needed, in particular because typically immortal cell lines also originating from non-respiratory (and often non-human) tissue are being used in early preclinical studies. For example, VeroE6, a widely used cell line in SARS-CoV-2 studies is defective in the expression of main the SARS-CoV-2 receptors (angiotensin-converting enzyme 2 (ACE2) and transmembrane protease serine 2 (TMPRSS2)). Hence, screenings campaigns often result in the discovery of antiviral agents that regulate autophagy pathways and endosomal-lysosomal maturation which may not be pertinent or translatable as SARS-CoV-2 therapies[2]. Meanwhile, air-liquid interface of differentiated primary human airway epithelial cells (HAEC) possess the architecture and cellular complexity of human lung tissue and are permissive to variety of respiratory viral infections[3,4]. Containing all relevant cell types of the lower respiratory tract (ciliated, goblet and basal cells) which includes ACE2 and TMPRSS2 expressing cells, this system allows to dissect the host-pathogen interactions at the molecular and cellular levels and provides a platform for the profiling of antiviral drugs.

In this study, we explored the effect of a selected number of reported SARS-CoV-2 inhibitors in HAEC ALI cultures on the replication of different SARS-CoV-2 isolates. Our results provide a reference set of data for the preclinical development of SARS-CoV-2 inhibitors.

MATERIALS AND METHODS

Cells and virus isolates

The African monkey kidney cell line VeroE6 tagged green fluorescent protein (VeroE6-GFP, kindly provided by M. van Loock, Janssen Pharmaceutica, Beerse, Belgium) and VeroE6 were maintained in Dulbecco's modified Eagle's medium (DMEM; Gibco, catalogue no. 41965-039) supplemented with 10% v/v heat-inactivated foetal bovine serum (HI-FBS; HyClone, catalogue no. SV03160.03), 1% v/v sodium bicarbonate 7.5% w/v ($NaHCO_3$; Gibco, catalogue no. 25080-060), and 1% v/v Penicillin-Streptomycin 10000 U/mL (P/S; Gibco, catalogue no. 15140148) at 37◦C and 5% CO_2. The hepatocellular carcinoma cell line Huh7 (kindly provided by Ralf Bartenschlager, University of Heidelberg, Germany) was propagated in DMEM supplemented with 10% HI-FBS, 1% $NaHCO_3$, 1% P/S, 1% non-essential amino acids (NEAA; Gibco, catalogue no. 11140050), and 2% HEPES 1M (Gibco, catalogue no. 15630106) at 37◦C and 5% CO_2. All assays involving virus growth were performed in the respective cell growth medium containing 2% (VeroE6-GFP) or 4% (Huh7) instead of 10% FBS.

SARS-CoV-2 isolate BetaCoV/Germany/BavPat1/2020 (EPI_ISL_406862|2020-01-28, kindly provided by C. Drosten, Charité, Berlin, Germany) and BetaCov/Belgium/GHB-03021/2020 (EPI_ISL_407976|2020-02-03) retrieved from RT-qPCR-confirmed COVID-19 positive patients in January and February 2020 were described previously[5,6]. The generation of virus stocks by serial passaging in Huh-7 and VeroE6 cells were fully reported[7,8]. BavPat1 isolate (passage 2 (P2)) and GHB-03021 isolate (P6 and P7) were used for the air liquid-interface experiment while only the latter was used for standard *in vitro* assays in VeroE6-GFP cells (P6 and P7) and in Huh7 cells (P9). The genomic sequence of both isolates is highly similar. BavPat1 carries the D614G amino acid change in the spike-protein while the GHB-03021 has a ΔTQTNS deletion at 676-680 residues that is typical for SARS2 strains that have been passaged several times on VeroE6 cells. All infectious virus-containing works were conducted in biosafety level 3 (BSL-3) and 3+ (CAPs-IT) facilities at the Rega Institute for Medical Research, KU Leuven, according to institutional guidelines.

Compounds

GS-441524 and EIDD-1931 were purchased from Carbosynth (United Kingdom) and R&D Systems (USA) respectively. Stock solutions (10 mM) were prepared using analytical grade dimethyl sulfoxide (DMSO). AT-511 was provided by Dr. A. Chatterjee from the California Institute for Biochemical Research (Calibr) (La Jolla, CA) and used as a 10 mM DMSO solution. The antiviral activity of AT-511 was confirmed on hepatitis C (data not shown). IFN λ1 was purchased from R&D Systems and IFN β-1a was a kind gift from the laboratory of Immunobiology (Rega Institute, KU Leuven, Belgium), which were reconstituted in sterile phosphate buffered saline (PBS, Life Technologies) containing at least 0.1% FBS.

In vitro standard antiviral and toxicity assays

VeroE6-GFP cells were seeded at a density of 25000 cells/well in 96-well plates (Greiner Bio One, catalogue no. 655090) and pre-treated with three-fold serial dilutions of the compounds overnight. On the next day (day 0), cells were infected with the SARS-CoV-2 inoculum at a multiplicity of infection (MOI) of 0.001 median tissue infectious dose (TCID50) per cell. The number of fluorescent pixels of GFP signal determined by High-Content Imaging (HCI) on day 4 post-infection (p.i.) was used as a read-out. Percentage of inhibition was calculated by subtracting background (number of fluorescent pixels in the untreated-infected control wells) and normalizing to the untreated-uninfected control wells (also background subtracted). The 50% effective concentration (EC_{50}, the concentration of compound required for fifty percent recovery of cell-induced fluorescence) was determined using logarithmic interpolation. Potential toxicity of compounds was assessed in a similar set-up in treated-uninfected cultures where metabolic activity was quantified at day 5 using the MTS assay as described earlier[9]. The 50% cytotoxic

concentration (CC_{50}, the concentration at which cell viability reduced to 50%) was calculated by logarithmic interpolation.

Huh7 cells were pre-seeded at 6000 cells/well in 96 well-plates (Corning, catalogue no.3300) and incubated overnight at 37◦C and 5% CO_2. On day 0, cells were firstly treated with the three-fold serial dilution of a potential antiviral, followed by either the inoculation of SARS-CoV-2 at MOI of 0.0037 TCID50/cell or addition of fresh medium. After 4 days, differences in cell viability caused by virus-induced cytopathic effect (CPE) or by compound-specific toxicity were evaluated using MTS assays. The EC_{50} and CC_{50} were calculated as above-mentioned.

Viral infection of reconstituted human airway epithelium cells

Tracheal HAEC (catalogue no. EP01MD) and human small airway epithelium cells (HsAEC) (catalogue no. EP21SA) from healthy donors were obtained from Epithelix (Geneva, Switzerland) in an air-liquid interphase set-up. After arrival, the insert was washed with pre-warmed 1x PBS (Gibco, catalogue no. 14190-094) and maintained in corresponding MucilAir medium (Epithelix, catalogue no. EP04MM) or SmallAir medium (Epithelix, catalogue no. EP64SA) at 37◦C and 5% CO_2 for at least 4 days before use. On the day of the experiment, the H(s)AEC were first pre-treated with basal medium containing compounds at different concentrations for indicated hours, followed by exposing to 100 µL of SARS-CoV-2 inoculum from apical side for 1.5 hours. Then the cultures were incubated at the indicated temperatures. The first apical wash with PBS was collected either right after the removal of viral inoculum (day 0) or 24 hours later (day 1 post-infection (p.i.)). Every other day from day 0, subsequent apical washes were collected whereas compound-containing medium in the basolateral side of the H(s)AEC culture was refreshed. Wash fluid was stored at -80◦C for following experiments.

RNA extraction and quantitative reverse transcription-PCR (RT-qPCR)

Viral RNA in the apical wash was isolated using the Cells-to-cDNA™ II cell lysis buffer kit (Thermo Fisher Scientific, catalogue no. AM8723). Briefly, 5 µL wash fluid was added to 50 µL lysis buffer, incubated at room temperature (RT) for 10 min and then at 75◦C for 15 min. 150 µL nuclease-free water was additionally added to the mixture prior to RT-qPCR. In parallel, a ten-fold serial dilution of corresponding virus stock was extracted. The amount of viral RNA expressed as TCID50 equivalent per insert (TCID50e/insert) was quantified by RT-qPCR using iTaq universal probes one-step kit (Bio-Rad, catalogue no. 1725141), and a commercial mix of primers for N gene (forward primer 5'-GACCCCAAAATCAGCGAAAT-3', reverse primer 5'-TCTGGTTACTGCCAGTTGAATCTG-3') and probes (5'-FAM-ACCCCGCATTACGTTTGGTGGACC-BHQ1-3') manufactured at IDT Technologies (catalogue no. 10006606). The reaction (final volume: 20 µL) consisted of 10 µL one-step reaction mix 2X , 0.5 µL reverse transcriptase, 1.5 µL of primers and probes mix, 4 µL nuclease-free water, and 4 µL viral RNA. The RT-qPCR was executed on a Lightcycler 96 thermocycler (Roche), starting at 50◦C for 15 min and 95◦C for 2 min, followed by 45 cycles of 3 sec at 95◦C and 30 sec at 55◦C.

Titration using a 50% tissue culture infectious dose (TCID50) assay

VeroE6 cells were seeded in 96-well tissue culture plates at a density of 1×10^4 cells/180 µL/well. After 24 hours, serial 10-fold dilutions of ALI wash fluid were prepared in the plates. Cells were incubated for 3 days at 37°C and evaluated microscopically for the absence or presence of virus induced cytopathic effect (CPE). The infectious viral titer was determined by end-point titration, expressed as TCID50/ml. Virus titers were calculated by using the Spearman and Karber method as previously reported[10,11].

Statistical analysis

All statistical comparisons in the study were performed in GraphPad Prism (GraphPad Software, Inc.). Statistical significance was determined using the ordinary one-way ANOVA with Dunnett's multiple comparison test. P-values of ≤0.05 were considered significant.

138 **RESULTS**

139 **Replication kinetics of SARS-CoV-2 in reconstituted human airway epithelia**

140 We first compared the replication kinetics of the Belgian isolate GHB-03021 and the German isolate
141 BavPat1. The main differences in the genomes of these viruses is the D614G amino acid change in the
142 spike-protein of BavPat1 and the deletion of several amino acids near the furin-cleavage site in the GHB-
143 03021 isolate (because of extensive passaging in VeroE6 cells). The replication kinetics was investigated
144 at respectively 35 and 37°C in both cultures from tracheal cells (HAEC) or from small airway cells (HsAEC).
145 In preliminary experiments, it was observed that an input of 10^2, 10^3 or 10^4 TCID50/insert resulted in
146 comparable levels of virus production (data not shown). We therefore selected 2×10^3 TCID50/insert as
147 the viral input for this experiment. Overall, BavPat1 infected the cultures more efficiently than the GHB-
148 03021 isolate did (Fig. 1). For example, at 37°C not all bronchiole-airway derived inserts infected with
149 GHB-03021 resulted in a productive infection whereas all cultures infected with BavPat1 showed
150 productive infection under all conditions. Virus replication was for both isolates higher at 35°C and more
151 reproducible as compared with a temperature of 37°C. This difference was more pronounced for the
152 HsAEC than for the HAEC cultures.

153

154 **Effect of selected antivirals on SARS-CoV-2 replication in HAEC cultures.**

155 Three nucleoside analogues that are known as inhibitors of SARS-CoV-2 replication were selected as
156 reference for studies in HAEC cultures. These included GS-441524[12-16] (the parent nucleoside of RDV),
157 EIDD-1931[16-18] (the active metabolite of Molnupiravir) and AT-511[17] [a guanosine nucleotide analogue
158 with activity against hepatitis C virus (HCV)]. In order to select a suitable concentration range of these
159 molecules to be used in the HAEC cultures, we first explored their effect in VeroE6 and Huh7 cell lines.
160 Both GS-441524 and EIDD-1931 selectively inhibited SARS-CoV-2 replication. On the other hand, AT-511
161 was surprisingly entirely devoid of antiviral activity (Table 1).

162 At 10 µM, GS-441524 sterilized the HAEC cultures from the GHB-03021 virus. Indeed, no virus production
163 was detected during the first 9 days of treatment and when treatment was stopped, no rebound was
164 observed over the next 5 days of culturing. When evaluated at a concentration of 1 µM, GS-441524
165 reduced virus yield by ~1 $\log_{10}$ during the time of treatment, but lost activity once the compound was
166 removed from the culture. In a separate experiment, GS-441524 at 3 µM resulted in complete inhibition
167 of virus production upon infection with BavPat1 (Fig. 2F-H). Also, 10 µM of EIDD-1931 resulted in a
168 pronounced antiviral effect (Fig. 3F-J). AT-511, however, at the various concentrations tested (1 and 10
169 µM) was devoid of an antiviral effect (Fig. 3A-E).

170 **Prophylactic interferon type I and type III reduce SARS-CoV-2 production**

171 Human IFN has been used to treat several viral infections[19,20] and recently clinical trialsagainst SARS-CoV-
172 2 are ongoing (ClinicalTrials.gov number: NCT04315948, NCT04385095, and NCT04492475). Therefore,
173 we investigated whether IFN β-1a and IFN λ1 exert activity when used as a prophylactic monotherapy.
174 Tracheal cultures were pre-treated with either 5 and 50 ng/mL IFN λ1 (5 ng/mL is the average
175 concentration secreted in the basal medium of infected HAEC cultures[21]) or 1 and 100 IU/mL IFN β-1a for
176 24 hours, and subsequently infected with BavPat1. Both drugs were able to reduce viral titers in a dose-
177 dependent manner (Fig. 4A, 4F). Viral loads were reduced by 100 IU/mL IFN β-1a (3.3 $\log_{10}$ vRNA
178 reduction, 3.6 $\log_{10}$ titer reduction) and 50 ng/mL IFN λ1 (4.2 logs vRNA reduction, 5.0 $\log_{10}$ titer reduction)
179 on day 4 p.i. (Fig. 4B, 4D, 4G, 4I respectively). At later time points viral load in the treated samples
180 increased again.

181

182 **DISCUSSION**

183 We demonstrate that *ex vivo* models reconstituted from human tracheal or small airway epithelium are
184 permissive for SARS-CoV-2 infection and robustly produces viral progenies from the apical side in long-
185 term experiments (up to 14 days p.i.). Recent studies report on the effect of different SARS-CoV-2 isolates
186 and incubation temperatures on virus replication kinetics[22-25]. We used two isolates, BavPat1 and GHB-
187 03021, whereby the BavPat1 provedto be more readily infectious. The BavPat1 isolate carries the p.D614G
188 substitution in the spike (S) protein while the GHB-03021 has a deletion of several amino-acids in the
189 S1/S2 boundary that is typically found in a VeroE6-adapted isolates[7]. The spike substitution D614G has
190 been reported to increase the stability and infectivity of virions in HAEC culture by enhancing the ACE2-
191 receptor-binding[26,27]. Isolates with this substitution have become globally dominant[26-29]. Meanwhile, it has
192 been noted that the continued propagation of SARS-CoV-2 in Vero cells causes several substitutions or
193 deletions in the S1/S2 boundary[25,30-33], which are only rarely observed in clinical samples[31,32]. We speculate
194 that the adaptation to Vero cells results in a phenotype that allows more efficient entry through an ACE2-
195 independent pathway. This entry mechanism would enhance entry in VeroE6 cells but would limit entry
196 in primary lung epithelial cells. Further mechanistic studies are required to elucidate this hypothesis.

197 The anatomical distance and ambient temperature between upper and lower human respiratory tracts
198 have a profound influence on the replication kinetics of respiratory viruses[22,34-36]. In agreement with other
199 studies, we observed SARS-CoV-2 growth in favour of lower temperature (35°C) which can be attributed
200 to the temperature preference of SARS-CoV-2 S protein for its folding and transport[24,37]. Altogether, both
201 primary HAEC and HsAEC cultures are shown to be a robust model for SARS-CoV-2 replication that can be
202 used for antiviral drug profiling.

203 A promising target for the development of novel antiviral agents active against coronaviruses is the viral
204 RNA-dependent RNA polymerase (RdRp)[38]. Remdesivir, a phosphoramidate prodrug of an adenosine C-
205 nucleoside, has been approved as the first COVID-19 therapy. However, its effectiveness is still a matter
206 of debate[1]. In addition, it has a challenging pharmacological profile allowing intravenous administration
207 only[39-41]. We demonstrate that the parent nucleoside GS-441524[12-16] can "sterilize" H(s)AEC cultures from
208 SARS-CoV2 as no rebound of the virus was noted several days after removal of the molecule. Differences
209 in antiviral potencies of RDV and GS-441524 have been reported depending on the cell lines used, which
210 correlates with the formation of the biologically active (5'-triphosphate) metabolite[12,13]. Data from a
211 pharmacokinetic study in mice suggests that GS-441524 could possibly be considered as an oral drug[12].

212 AT-527 is currently being evaluated in phase II clinical trials for COVID-19 (ClinicalTrials.gov). Surprisingly,
213 we did not observe anti-SARS-CoV-2 activity of AT-511, the free base form of AT-527, in VeroE6 and Huh7
214 cells, nor did we observe antiviral activity in the HAEC cultures. This is in contrast with a recent publication
215 where sub-micromolar activities of AT-511 were observed in very similar assay systems[17]. At this moment
216 we have no explanation for this discrepancy. One possibility is that small differences in the assay
217 conditions may influence the metabolization of AT-511 to its active form and thus influence its antiviral
218 activity. As AT-511 is a double pro-drug it may be more susceptible to these nuances.

219 In addition to RDV and AT-511, we also investigated the effect of the nucleoside analogue EIDD-1931
220 which is the active metabolite of the ester prodrug Molnupiravir (EIDD-2801). EIDD-1931 has been
221 reported to exert antiviral activity against various human coronaviruses and Molnupiravir is currently in
222 clinical trials for SARS-CoV-2[17,18]. Initial interim data from a phase II study provides first evidence for
223 antiviral activity in COVID patients (https://www.croiconference.org/abstract/reduction-in-infectious-
224 sars-cov-2-in-treatment-study-of-covid-19-with-molnupiravir/). Like GS-441524, EIDD-1931 also results in

225 a pronounced antiviral effect in the human airway epithelium cell cultures, which is consistent with
226 another report[18].

227 Also, a significant inhibitory effect of IFN β-1a and IFN λ1 was noted, although at high concentrations and
228 in particular during the first days of the treatment. At later time-points, viral replication increased in the
229 treated cultures, suggesting that the virus can escape the effect of IFN. The effective concentration of IFN
230 β-1a used in this study is comparable with the clinically achievable concentration and is in line with other
231 reports[19,20,42].

232 In conclusion, we assessed (i) the replication of two SARS-CoV-2 isolates in H(s)AEC cultures and (ii) the
233 antiviral effect of a selected list of inhibitors. These data provide a reference when developing yet other
234 inhibitors of SARS-CoV2 replication.

235 Acknowledgements

236 We thank Birgit Voeten, Niels Cremers, Tina van Buyten and Thibault Francken for their excellent technical
237 assistance. We also thank Piet Maes for kindly providing the SARS-CoV-2 GHB-03021/2020 isolateused in
238 this study. This research was supported by Bill & Melinda Gates Foundation (BMGF) under grant number
239 INV-006366. T.N.D.D received the fellowship from European Union's Horizon 2020 research and
240 innovation programme under Marie Sklodowska-Curie grant agreement No. 812673 (OrganoVIR project).
241 Part of this research work was performed using the 'Caps-It' research infrastructure (project ZW13-02)
242 that was financially supported by the Hercules Foundation and Rega Foundation, KU Leuven.

243 Conflict of interest

244 All authors declare that there is no conflict of interest.

245 Author contributions

246 J.N. and D.J. conceptualized and supervised the project. T.N.D.D and D.J. designed the research. T.N.D.D.
247 performed the ALI-related experiments. T.N.D.D. analysed data. A.J.C, P.A.G, and M.D.B. characterized
248 AT-511 structure and tested its activity against HCV. T.N.D.D. wrote the first draft of the manuscript. D.J.,
249 S.D.J., L.V., and J.N. edited the manuscript. L.V., D.J. and J.N. acquired the funding.

250

251

Reference

1. Consortium WHOST, Pan H, Peto R, et al. Repurposed Antiviral Drugs for Covid-19 - Interim WHO Solidarity Trial Results. *N Engl J Med.* 2021;384(6):497-511.
2. Murgolo N, Therien AG, Howell B, et al. SARS-CoV-2 tropism, entry, replication, and propagation: Considerations for drug discovery and development. *PLoS Pathog.* 2021;17(2):e1009225.
3. Boda B, Benaoudia S, Huang S, et al. Antiviral drug screening by assessing epithelial functions and innate immune responses in human 3D airway epithelium model. *Antiviral Res.* 2018;156:72-79.
4. Loo SL, Wark PAB, Esneau C, Nichol KS, Hsu AC, Bartlett NW. Human coronaviruses 229E and OC43 replicate and induce distinct antiviral responses in differentiated primary human bronchial epithelial cells. *Am J Physiol Lung Cell Mol Physiol.* 2020;319(6):L926-L931.
5. Bohmer MM, Buchholz U, Corman VM, et al. Investigation of a COVID-19 outbreak in Germany resulting from a single travel-associated primary case: a case series. *Lancet Infect Dis.* 2020;20(8):920-928.
6. Dellicour S, Durkin K, Hong SL, et al. A Phylodynamic Workflow to Rapidly Gain Insights into the Dispersal History and Dynamics of SARS-CoV-2 Lineages. *Mol Biol Evol.* 2020.
7. Boudewijns R, Thibaut HJ, Kaptein SJF, et al. STAT2 signaling restricts viral dissemination but drives severe pneumonia in SARS-CoV-2 infected hamsters. *Nat Commun.* 2020;11(1):5838.
8. Rut W, Groborz K, Zhang L, et al. SARS-CoV-2 M(pro) inhibitors and activity-based probes for patient-sample imaging. *Nat Chem Biol.* 2021;17(2):222-228.
9. Jochmans D, Leyssen P, Neyts J. A novel method for high-throughput screening to quantify antiviral activity against viruses that induce limited CPE. *J Virol Methods.* 2012;183(2):176-179.
10. Kärber G. Beitrag zur kollektiven Behandlung pharmakologischer Reihenversuche. *Naunyn-Schmiedebergs Archiv für experimentelle Pathologie und Pharmakologie.* 1931;162(4):480-483.
11. Spearman C. The method of 'right and wrong cases' ('constant stimuli') without Gauss's formulae. *British Journal of Psychology.*2:227-242.
12. Li Y, Cao L, Li G, et al. Remdesivir Metabolite GS-441524 Effectively Inhibits SARS-CoV-2 Infection in Mouse Models. *Journal of Medicinal Chemistry.* 2021.
13. Pruijssers AJ, George AS, Schafer A, et al. Remdesivir Inhibits SARS-CoV-2 in Human Lung Cells and Chimeric SARS-CoV Expressing the SARS-CoV-2 RNA Polymerase in Mice. *Cell Rep.* 2020;32(3):107940.
14. Shi Y, Shuai L, Wen Z, et al. The Preclinical Inhibitor GS441524 in Combination with GC376 Efficaciously Inhibited the Proliferation of SARS-CoV-2 in the Mouse Respiratory Tract. *bioRxiv.* 2020:2020.2011.2012.380931.
15. Xie X, Muruato AE, Zhang X, et al. A nanoluciferase SARS-CoV-2 for rapid neutralization testing and screening of anti-infective drugs for COVID-19. *Nat Commun.* 2020;11(1):5214.
16. Zandi K, Amblard F, Musall K, et al. Repurposing Nucleoside Analogs for Human Coronaviruses. *Antimicrob Agents Chemother.* 2020;65(1).
17. Good SS, Westover J, Jung KH, et al. AT-527, a double prodrug of a guanosine nucleotide analog, is a potent inhibitor of SARS-CoV-2 in vitro and a promising oral antiviral for treatment of COVID-19. *Antimicrob Agents Chemother.* 2021.
18. Sheahan TP, Sims AC, Zhou S, et al. An orally bioavailable broad-spectrum antiviral inhibits SARS-CoV-2 in human airway epithelial cell cultures and multiple coronaviruses in mice. *Sci Transl Med.* 2020;12(541).
19. Lokugamage KG, Hage A, de Vries M, et al. Type I Interferon Susceptibility Distinguishes SARS-CoV-2 from SARS-CoV. *J Virol.* 2020;94(23).

20. Strayer DR, Dickey R, Carter WA. Sensitivity of SARS/MERS CoV to interferons and other drugs based on achievable serum concentrations in humans. *Infect Disord Drug Targets.* 2014;14(1):37-43.
21. Essaidi-Laziosi M, Brito F, Benaoudia S, et al. Propagation of respiratory viruses in human airway epithelia reveals persistent virus-specific signatures. *J Allergy Clin Immunol.* 2018;141(6):2074-2084.
22. Corman VM, Eckerle I, Memish ZA, et al. Link of a ubiquitous human coronavirus to dromedary camels. *Proc Natl Acad Sci U S A.* 2016;113(35):9864-9869.
23. Pohl MO, Busnadiego I, Kufner V, et al. SARS-CoV-2 Variants Reveal Features Critical for Replication in Primary Human Cells. *bioRxiv.* 2021:2020.2010.2022.350207.
24. V'kovski P, Gultom M, Kelly J, et al. Disparate temperature-dependent virus – host dynamics for SARS-CoV-2 and SARS-CoV in the human respiratory epithelium. *bioRxiv.* 2020:2020.2004.2027.062315.
25. Zhu Y, Feng F, Hu G, et al. The S1/S2 boundary of SARS-CoV-2 spike protein modulates cell entry pathways and transmission. *bioRxiv.* 2020:2020.2008.2025.266775.
26. Korber B, Fischer WM, Gnanakaran S, et al. Tracking Changes in SARS-CoV-2 Spike: Evidence that D614G Increases Infectivity of the COVID-19 Virus. *Cell.* 2020;182(4):812-827.e819.
27. Yurkovetskiy L, Wang X, Pascal KE, et al. Structural and Functional Analysis of the D614G SARS-CoV-2 Spike Protein Variant. *Cell.* 2020;183(3):739-751 e738.
28. Plante JA, Liu Y, Liu J, et al. Spike mutation D614G alters SARS-CoV-2 fitness. *Nature.* 2020.
29. Zhang L, Jackson CB, Mou H, et al. The D614G mutation in the SARS-CoV-2 spike protein reduces S1 shedding and increases infectivity. *bioRxiv.* 2020.
30. Davidson AD, Williamson MK, Lewis S, et al. Characterisation of the transcriptome and proteome of SARS-CoV-2 reveals a cell passage induced in-frame deletion of the furin-like cleavage site from the spike glycoprotein. *Genome Medicine.* 2020;12(1):68.
31. Lau SY, Wang P, Mok BW, et al. Attenuated SARS-CoV-2 variants with deletions at the S1/S2 junction. *Emerg Microbes Infect.* 2020;9(1):837-842.
32. Liu Z, Zheng H, Lin H, et al. Identification of Common Deletions in the Spike Protein of Severe Acute Respiratory Syndrome Coronavirus 2. *J Virol.* 2020;94(17).
33. Ogando NS, Dalebout TJ, Zevenhoven-Dobbe JC, et al. SARS-coronavirus-2 replication in Vero E6 cells: replication kinetics, rapid adaptation and cytopathology. *J Gen Virol.* 2020;101(9):925-940.
34. Tyrrell DA, Bynoe ML. CULTIVATION OF A NOVEL TYPE OF COMMON-COLD VIRUS IN ORGAN CULTURES. *Br Med J.* 1965;1(5448):1467-1470.
35. Holwerda M, Kelly J, Laloli L, et al. Determining the Replication Kinetics and Cellular Tropism of Influenza D Virus on Primary Well-Differentiated Human Airway Epithelial Cells. *Viruses.* 2019;11(4):377.
36. Kendall EJ, Bynoe ML, Tyrrell DA. Virus isolations from common colds occurring in a residential school. *Br Med J.* 1962;2(5297):82-86.
37. Laporte M, Stevaert A, Raeymaekers V, et al. The SARS-CoV-2 and other human coronavirus spike proteins are fine-tuned towards temperature and proteases of the human airways. *bioRxiv.* 2020:2020.2011.2009.374603.
38. te Velthuis AJ. Common and unique features of viral RNA-dependent polymerases. *Cell Mol Life Sci.* 2014;71(22):4403-4420.
39. Sheahan TP, Sims AC, Graham RL, et al. Broad-spectrum antiviral GS-5734 inhibits both epidemic and zoonotic coronaviruses. *Sci Transl Med.* 2017;9(396):eaal3653.
40. Williamson BN, Feldmann F, Schwarz B, et al. Clinical benefit of remdesivir in rhesus macaques infected with SARS-CoV-2. *Nature.* 2020;585(7824):273-276.

41. Warren TK, Jordan R, Lo MK, et al. Therapeutic efficacy of the small molecule GS-5734 against Ebola virus in rhesus monkeys. *Nature.* 2016;531(7594):381-385.
42. Vanderheiden A, Ralfs P, Chirkova T, et al. Type I and Type III Interferons Restrict SARS-CoV-2 Infection of Human Airway Epithelial Cultures. *J Virol.* 2020;94(19).

350 ## Legends to the Figures

351 **Figure 1. SARS-CoV-2 replication kinetics in air-liquid interface cultures.** Viral replication of BavPat1 and GHB-03021 isolates at
352 2×10^3 TCID50/insert in human tracheal airway epithelia cells (A-D) or in human small airway epithelia cells (E-H) at either 35°C
353 (red circle) or 37°C (blue square) in comparison with uninfected control (black triangle). Viral RNA or infectious particles in apical
354 washes were quantified by RT-qPCR (A, C, E, G) or by end-point titrations (B, D, F, H), respectively. The results of individual inserts
355 are depicted as dots. The line follows the average of each conditions.

356 **Figure 2. GS-441524 blocks SARS-CoV-2 replication in primary human airway cultures.** Compounds were added to the basal
357 medium at different concentrations, starting from the in vitro EC50. The treatment period is illustrated in grey, initiating at 2
358 hours before infection. Viral RNA or infectious particles in apical washes were quantified by RT-qPCR (A-C, F-G) or by end-point
359 titrations (D-E, H), respectively. (A) Effect of GS-441524 at 10 and 1 µM on the replication of the GHB-03021 isolate. Tracheal
360 issues were infected with 2×10^4 TCID50/insert at 37°C. The viral production was compared between groups after 9 (B, D) or 14
361 days post-infection (C, E). (F) Activity of GS-441524 at 3 µM on the replication of the BavPat1 isolate. Small airway tissues were
362 infected with BavPat1 isolate at 2×10^3 TCID50/insert at 37°C. Viral production was compared between groups at the end of the
363 treatment (G-H). All data are mean ± SD of at least three independent ALI inserts. The dotted lines represent the lower limit of
364 detection (LLOD). Asterisks indicate a significant difference between treated samples and infected untreated control. *$p < 0.05$,
365 **$p < 0.01$, ***$p < 0.001$, ****$p < 0.0001$

366 **Figure 3. Antiviral activity of nucleoside analogues against SARS-CoV-2 in primary human tracheal airway cultures.** Compounds
367 were added to the basal medium at different concentrations, starting 1 hour before infection with BavPat1 isolate at 2×10^3
368 TCID50/insert at 37°C. Basal medium, with or without compounds, was refreshed every other day from day 0 to day 8. Viral RNA
369 or infectious particles in apical washes were quantified by RT-qPCR (A-C, F-H) or by end-point titrations (D-E, I-J), respectively.
370 Dose-response and time-dependent activity of AT-511 (A) and EIDD-1931 (F). Comparison of the viral production between groups
371 after 6 (B, D, G, I) or 8 days post-infection (C, E, H, J). All data are mean ± SD of at least three replicates. The dotted lines represent
372 the lower limit of detection (LLOD). Asterisks indicate a significant difference between treated samples and infected untreated
373 control. *$p < 0.05$, **$p < 0.01$, ***$p < 0.001$, ****$p < 0.0001$

374 **Figure 4. Prophylactic interferon type I and type III reduce SARS-CoV-2 production.** IFNs were added to the basal medium at
375 different concentrations 24 hours before infection with BavPat1 isolate (2×10^3 TCID50/insert at 37°C) and medium with or
376 without IFNs was refreshed every other day from day 0 to day 8. Viral RNA or infectious virions in apical washes were quantified
377 by RT-qPCR (A-C, F-H) or by end-point titrations (D-E, I-J), respectively. Dose-response and time-dependent activity of AT-511 (A)
378 and EIDD-1931 (F). The viral production was compared between groups after 4 (B, D, G, I) or 6 days post-infection (C, E, H, J). All
379 data are mean ± SD of at least three replicates. The dotted lines represent the lower limit of detection (LLOD). Asterisks indicate
380 a significant difference between treated samples and infected untreated control. *$p < 0.05$, **$p < 0.01$, ***$p < 0.001$, ****$p <$
381 0.0001

382

383

384 **Table 1. Antiviral activity against SARS-CoV-2 in cell culture**

Compounds	VeroE6-GFP			Huh-7		
	EC50 (µM)	CC50 (µM)	SI	EC50 (µM)	CC50 (µM)	SI
GS-441524	0.78 – 0.89	49 - 83	> 50	1.1 – 1.5	37 – 59	> 20
AT-511	> 100	> 100	ND	> 100	> 100	ND
EIDD-1931	0.57 – 0.87	> 100	> 100	1.3 – 1.4	11 - 12	8.5

385 Data represents the interquartile range (Q1-Q3) obtained from at least two independent experiments, each performed with
386 duplicate samples. Abbreviations: SI, selectivity index. ND: not determined

387

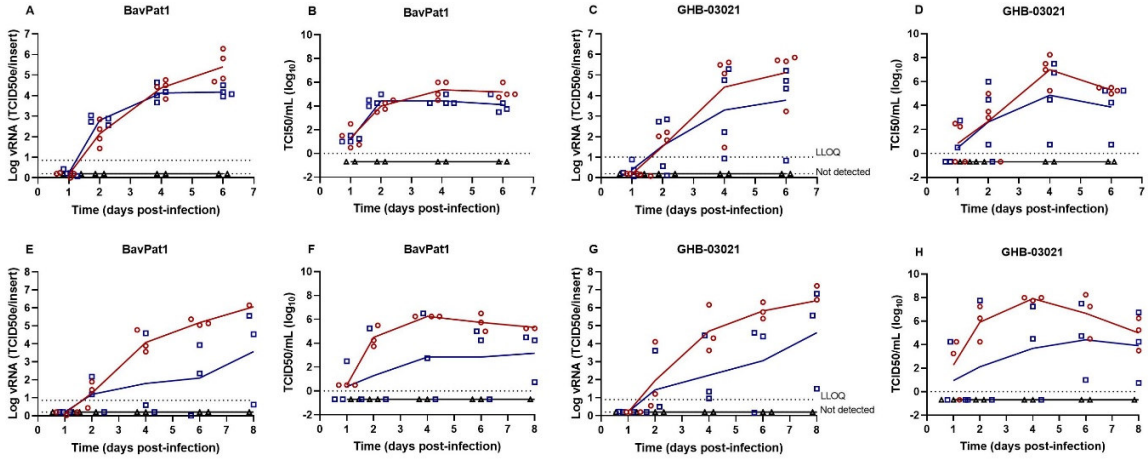
A
BavPat1
Log vRNA (TCID50e/insert)
Time (days post-infection)
B
BavPat1
TCI50/mL (log10)
Time (days post-infection)
C
GHB-03021
Log vRNA (TCID50e/insert)
LLOQ
Not detected
Time (days post-infection)
D
GHB-03021
TCI50/mL (log10)
Time (days post-infection)
E
BavPat1
Log vRNA (TCID50e/insert)
Time (days post-infection)
F
BavPat1
TCID50/mL (log10)
Time (days post-infection)
G
GHB-03021
Log vRNA (TCID50e/insert)
LLOQ
Not detected
Time (days post-infection)
H
GHB-03021
TCID50/mL (log10)
Time (days post-infection)

388

389

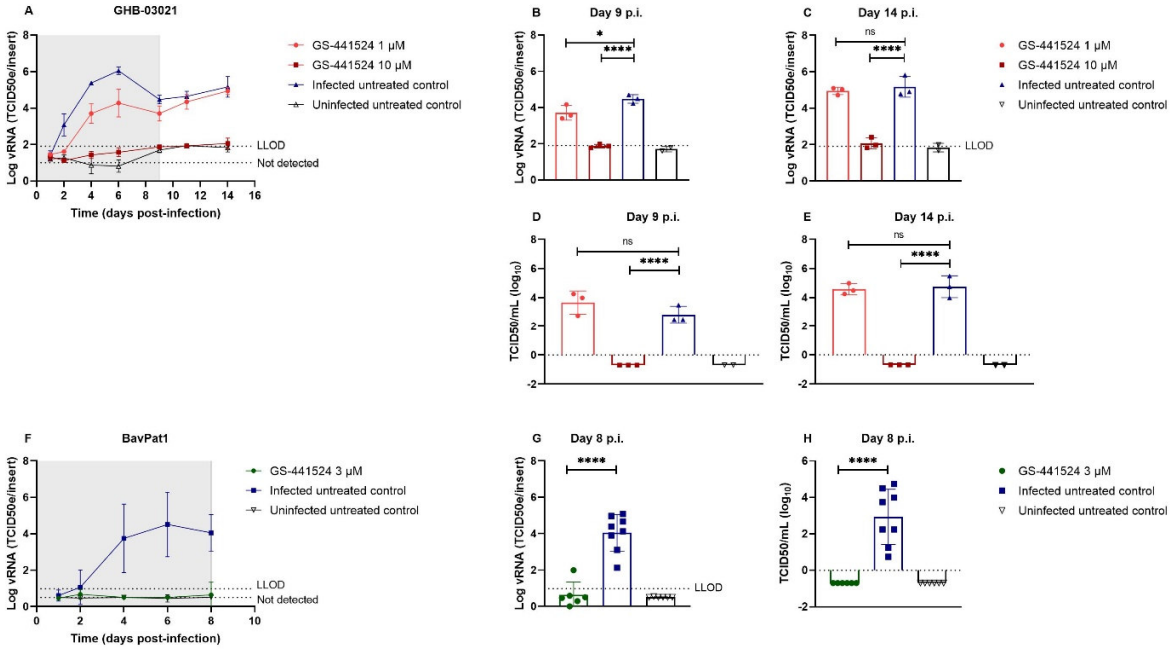
A
GHB-03021
Log vRNA (TCID50e/insert)
Time (days post-infection)
GS-441524 1 μM
GS-441524 10 μM
Infected untreated control
Uninfected untreated control
LLOD
Not detected
B
Day 9 p.i.
C
Day 14 p.i.
D
Day 9 p.i.
E
Day 14 p.i.
TCID50/mL (log10)
ns
F
BavPat1
GS-441524 3 μM
G
Day 8 p.i.
H
Day 8 p.i.

390

391

392

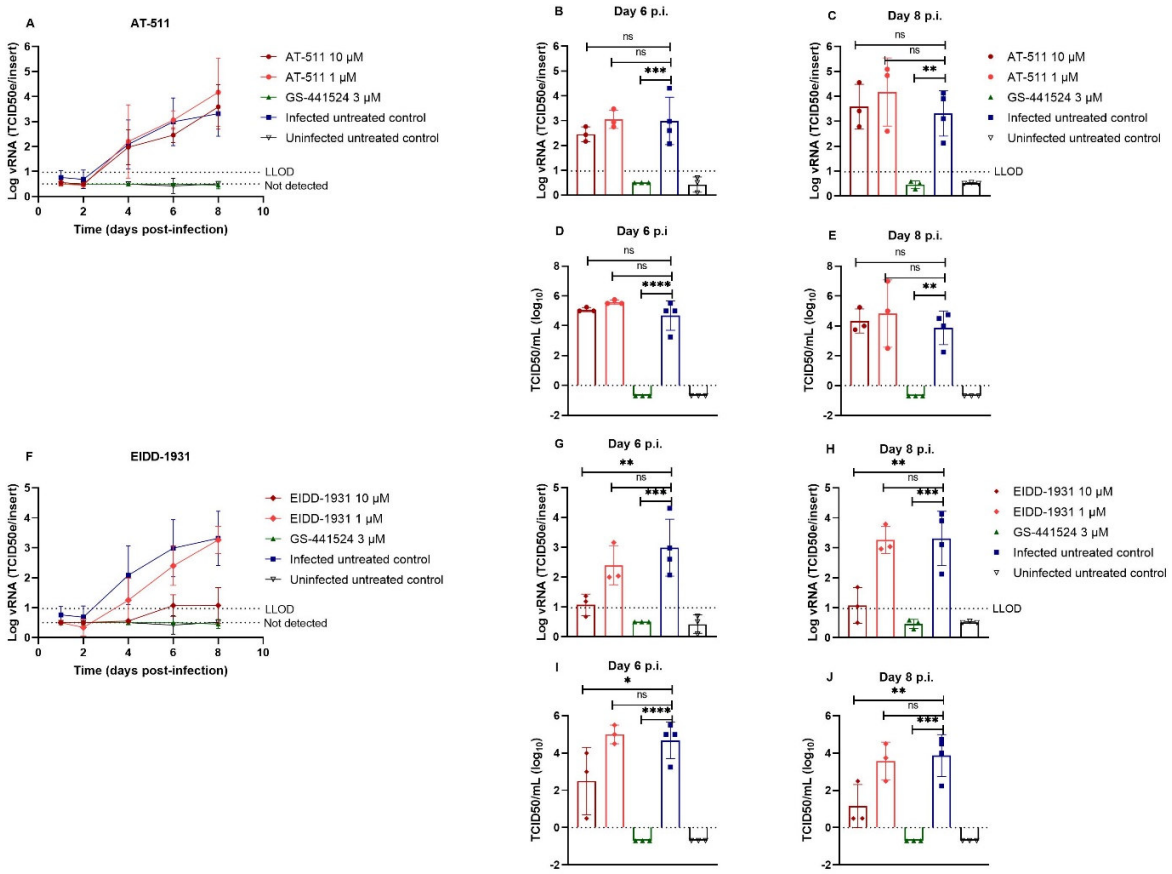
A
AT-511
Log vRNA (TCID50e/insert)
Time (days post-infection)
AT-511 10 μM
AT-511 1 μM
GS-441524 3 μM
Infected untreated control
Uninfected untreated control
LLOD
Not detected
B
Day 6 p.i.
C
Day 8 p.i.
D
Day 6 p.i
E
Day 8 p.i.
TCID50/mL (log10)
F
EIDD-1931
EIDD-1931 10 μM
EIDD-1931 1 μM
G
H
I
J
ns
*
**
***
****

393

394

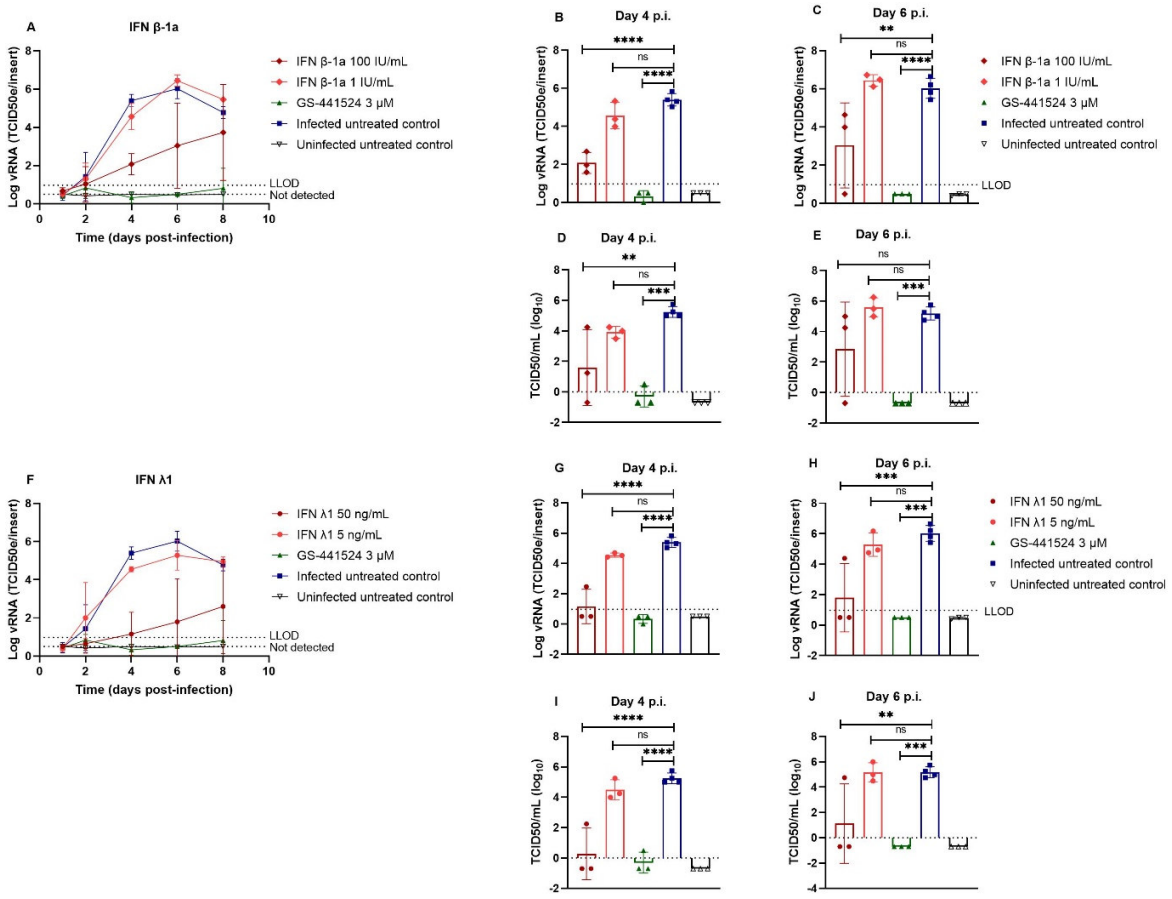
A
IFN β-1a
Log vRNA (TCID50e/insert)
Time (days post-infection)
IFN β-1a 100 IU/mL
IFN β-1a 1 IU/mL
GS-441524 3 μM
Infected untreated control
Uninfected untreated control
LLOD
Not detected
B
Day 4 p.i.
C
Day 6 p.i.
D
Day 4 p.i.
E
Day 6 p.i.
TCID50/mL (log10)
F
IFN λ1
IFN λ1 50 ng/mL
IFN λ1 5 ng/mL
G
Day 4 p.i.
H
Day 6 p.i.
I
Day 4 p.i.
J
Day 6 p.i.
ns

395